

# Measurement of higher moments of net-proton distributions in Au+Au collisions at $\sqrt{s_{NN}} = 54.4$ GeV at RHIC

Ashish Pandav (For the STAR collaboration)

National Institute of Science Education and Research,  
INDIA

## Outline

1. Introduction
2. Observable and Data Set
3. The STAR Experiment
4. Higher Moment Analysis
5. Results
6. Summary

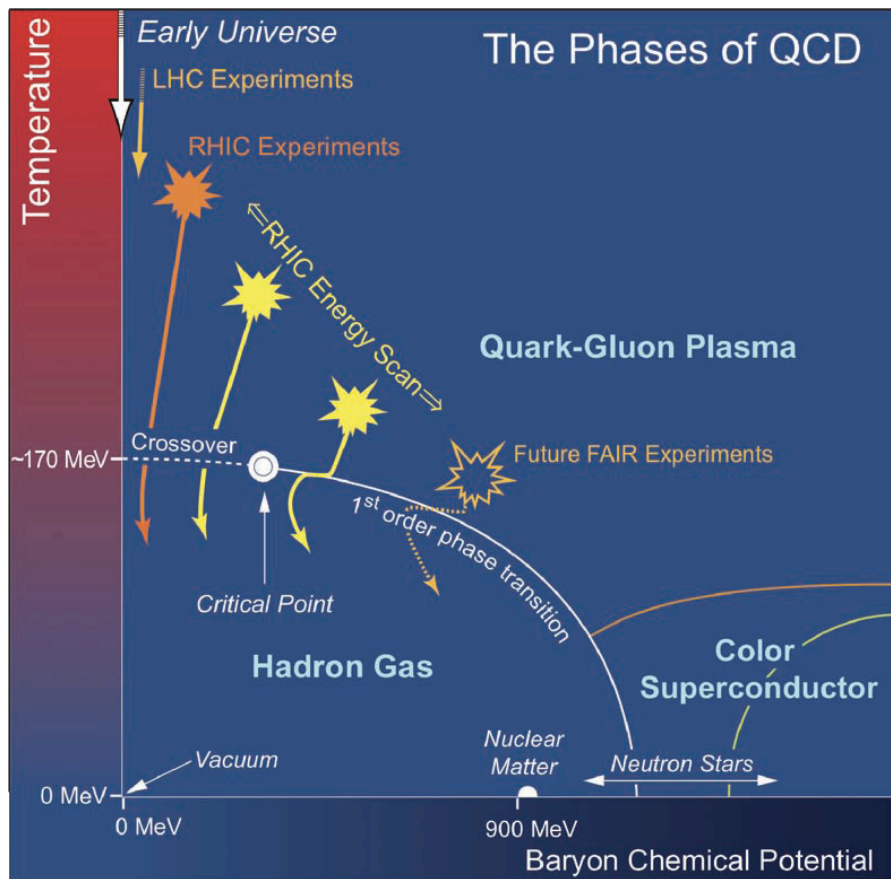


*XVIII International Conference on Strangeness in Quark Matter (SQM 2019)*

*Bari, Italy, 10-15 June 2019*



# Introduction: QCD Phase Diagram & BES



<https://drupal.star.bnl.gov/STAR/starnotes/public/sn0493>  
[https://drupal.star.bnl.gov/STAR/files/BES\\_WPII\\_ver6.9\\_Cover.pdf](https://drupal.star.bnl.gov/STAR/files/BES_WPII_ver6.9_Cover.pdf)

Goal: Study the phase diagram of QCD and the phase structure.

BES: Varying beam energy varies Temperature ( $T$ ) and Baryon Chemical Potential ( $\mu_B$ ).  
Fluctuations in various observables are sensitive to phase transition and critical point.

Results from new data : Au+Au collisions at  $\sqrt{s_{NN}} = 54.4$  GeV

# Observables



Higher moments or cumulants of net-particle distributions

$$C_1 = \langle N \rangle$$

$$C_2 = \langle (\delta N)^2 \rangle$$

$$C_3 = \langle (\delta N)^3 \rangle$$

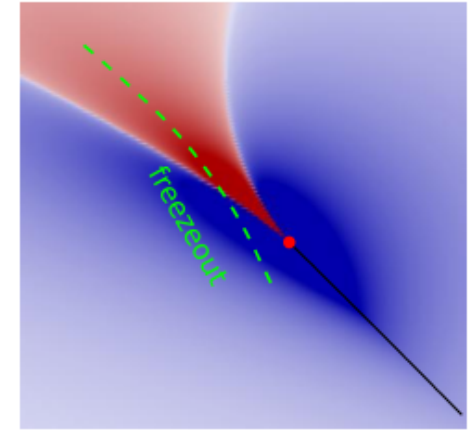
$$C_4 = \langle (\delta N)^4 \rangle - 3 \langle (\delta N)^2 \rangle^2$$

$$\sigma^2 / M = \frac{C_2}{C_1}$$

$$S\sigma = \frac{C_3}{C_2}$$

$$\kappa\sigma^2 = \frac{C_4}{C_2}$$

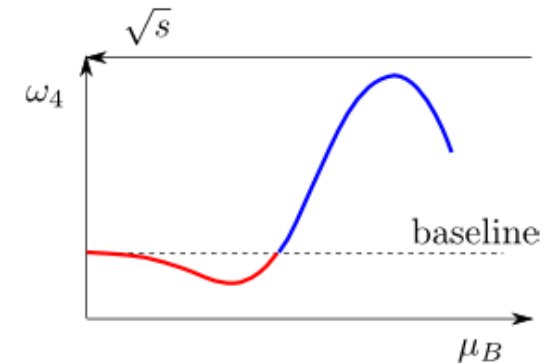
Kurtosis of net-proton in the presence of CP



Higher moments of conserved number distributions are sensitive observables.\* Related to the correlation length and susceptibilities.

$$\langle \sigma^2 \rangle \sim \xi^2 \quad \kappa_4 = \langle \sigma^4 \rangle_c \sim \xi^7$$

\*Quantitative numbers  
- Model dependent



- Phys.Rev.Lett. 107 (2011) 052301
- Phys.Rev.Lett. 102 (2009) 032301
- Phys.Rev.Lett. 91 (2003) 102003
- Phys.Rev.Lett. 81 (1998) 4816-4819
- Phys.Rev. D82 (2010) 074008
- Phys.Rev. D61 (2000) 105017
- Phys.Rev.Lett. 103 (2009) 262301

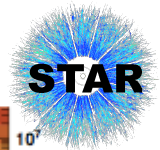
$$\frac{\chi_q^4}{\chi_q^2} = \kappa\sigma^2 = \frac{C_{4,q}}{C_{2,q}} \quad \frac{\chi_q^3}{\chi_q^2} = S\sigma = \frac{C_{3,q}}{C_{2,q}},$$

# Data Set

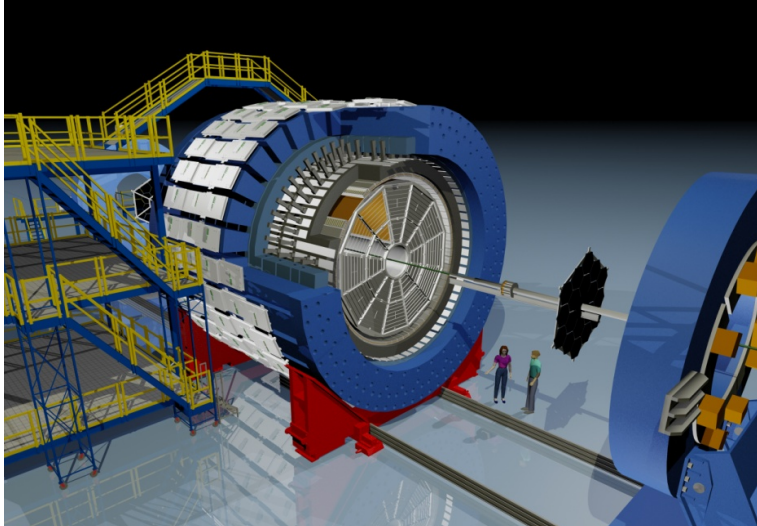


Collision system and energy	Au+Au and 54.4 GeV
Baryon Chemical Potential	~ 90 MeV
No. of events	~ 553 M
Collision centrality	0-5%, 5-10%, 10-20%, 20-30%, 30-40%, 40-50%, 50-60%, 60-70%, 70-80%
Centrality	$ \eta  < 1$ ; charged particles other than protons and antiprotons
Z Vertex	+/- 30 cm
Vertex radial position	2 cm
Detectors	Time Projection Chamber and Time-of-Flight
Particle Type	Proton and antiprotons
Rapidity	+/- 0.5
Transverse Momentum Range	0.4 to 2.0 GeV/c
Secondary proton backgrounds	$ DCA  < 1\text{cm}$

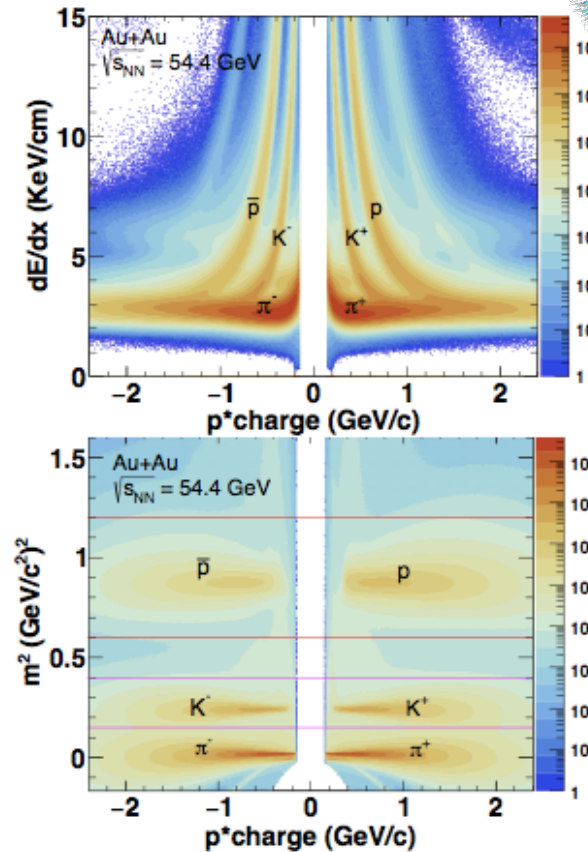
# The STAR Detector



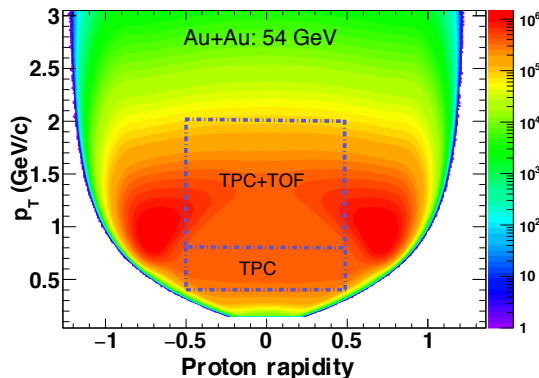
Nucl. Instrum. Meth. A 499, 624 (2003).



Main Detectors: Time Projection Chamber and Time-of-Flight  
**One unit rapidity coverage at mid-rapidity.**  
**Full azimuthal angle coverage.**



**Track-by-track PID** in each event  
 Purity > 96% for studied  $p_T$  range.



Collider: **Uniform acceptance** in  $p_T$  vs. rapidity at mid-rapidity for all particles.

STAR: Phys.Rev. C88 (2013) 014902  
 Phys.Rev. C81 (2010) 024911

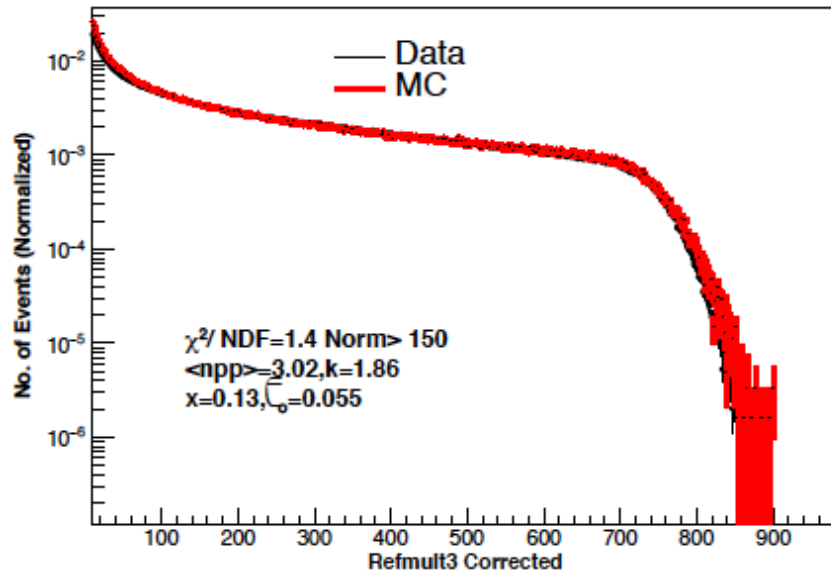
# Centrality Selection



Use charged particles other than protons and antiprotons within  $|\eta| < 1.0$ . Avoids auto-correlation effects

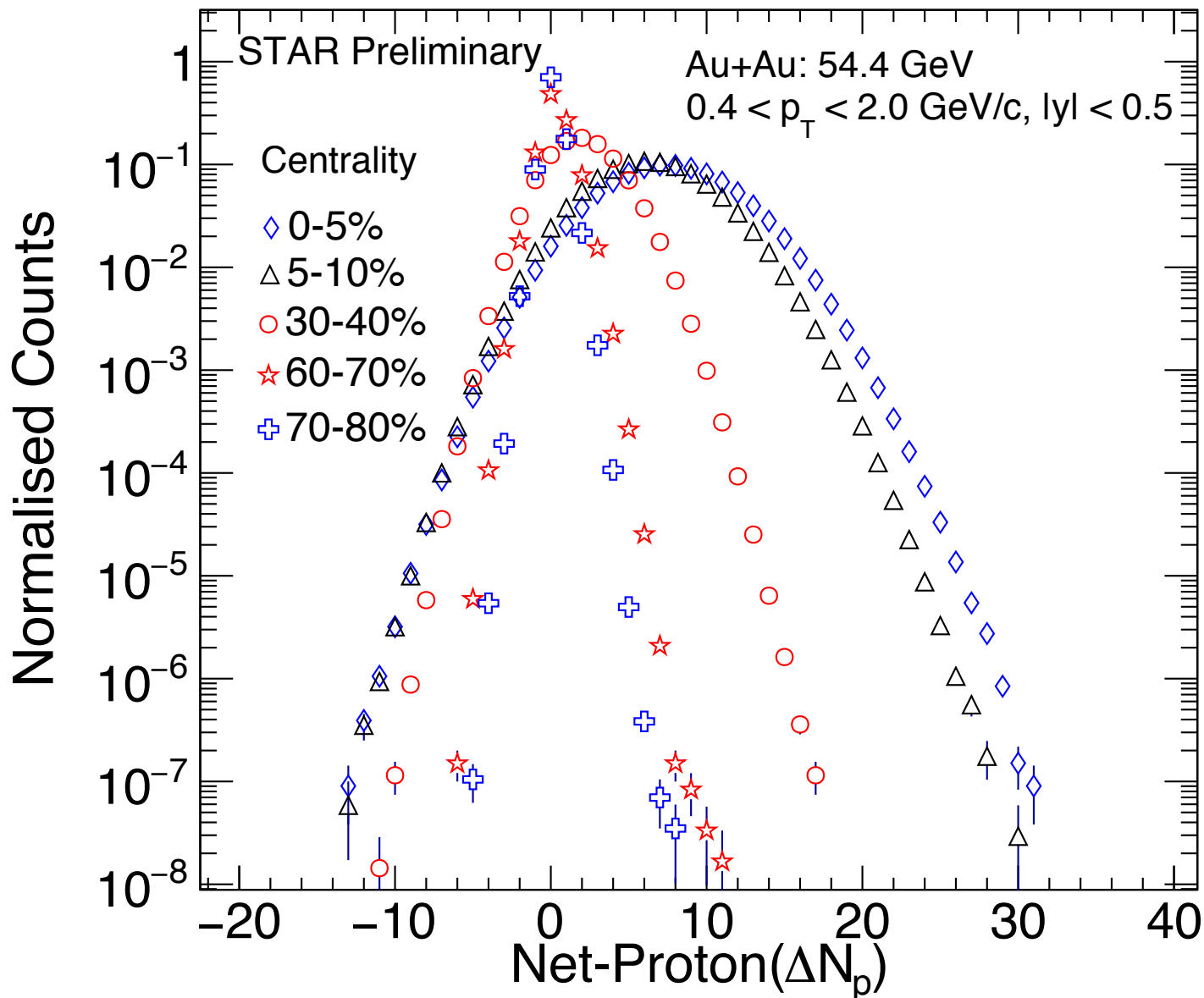
Corrected for luminosity and Z-vertex effects.

Compared to the MC Glauber model



Centrality	Refmult	Npart	Events (Millions)
0-5%	621	346	33
5-10%	516	292	34
10-20%	354	228	70
20-30%	237	161	69
30-40%	151	111	69
40-50%	90	73	67
50-60%	50	45	64
60-70%	24	26	60
70-80%	10	13	57

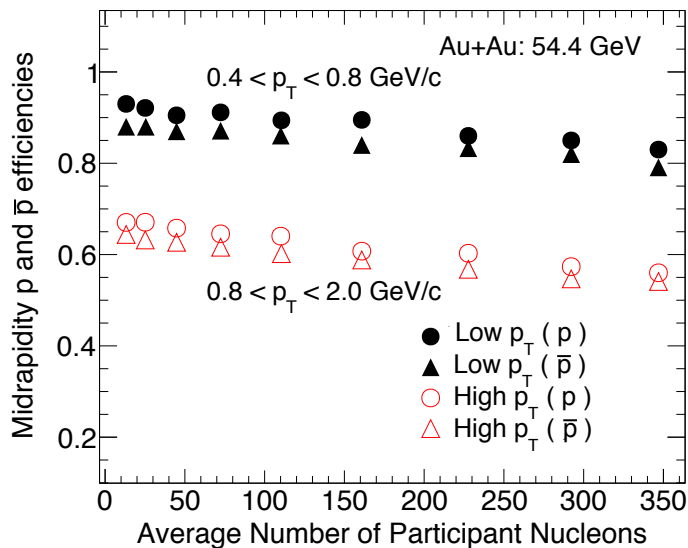
# Event-by-Event Distribution



# Corrections and Uncertainties



## Centrality Bin Width Correction



Statistical Uncertainties:  
Boot Strap Method

Sources of Systematic Uncertainties:  
Particle Identification  
Track Quality Cuts  
Background Estimates (DCA)

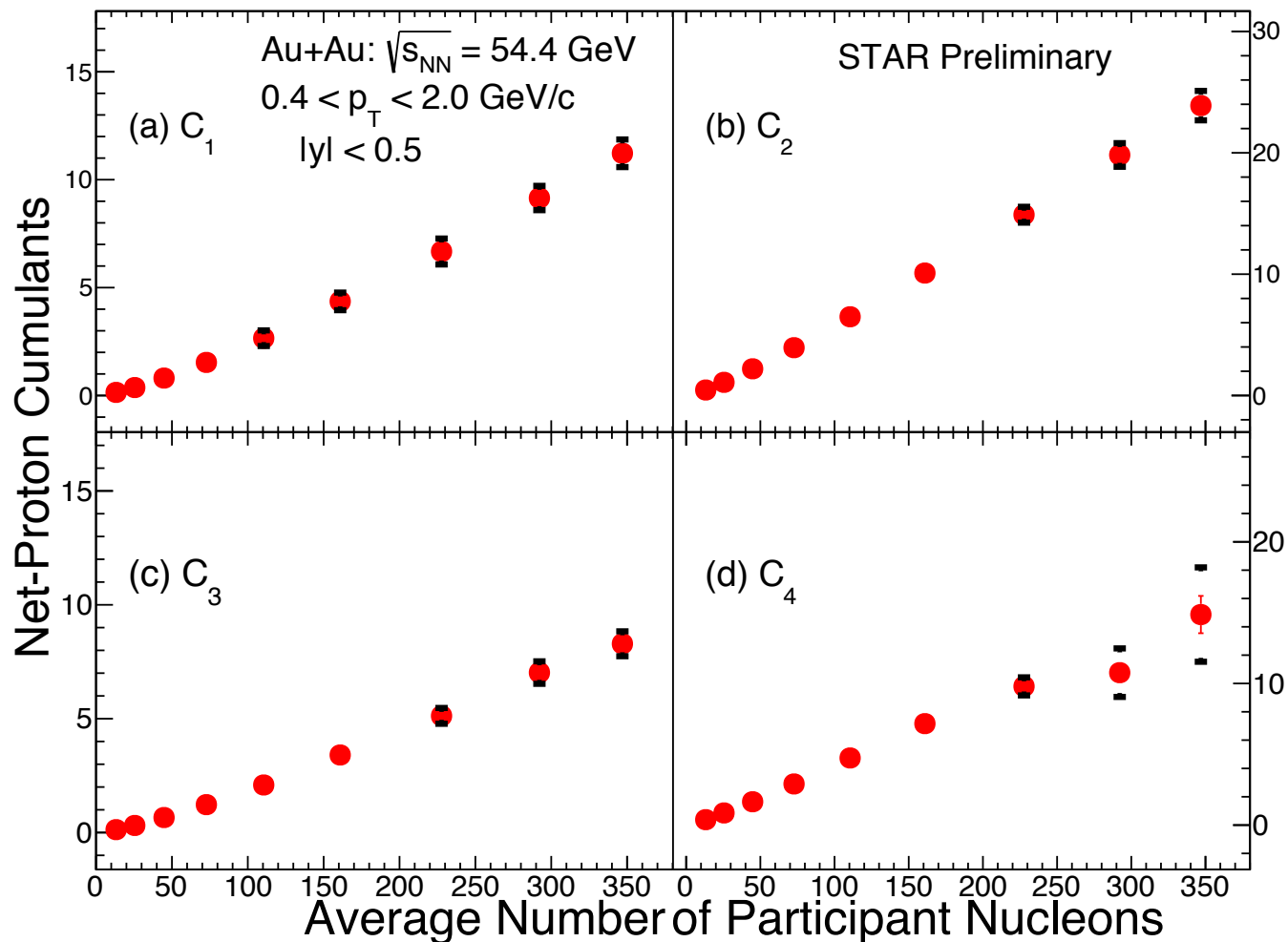
## Reconstruction Efficiency Correction - Binomial model

Cumulant	Stat. Uncertainties (0-5%)
$C_1$	0.008%
$C_2$	0.04%
$C_3$	1%
$C_4$	9%

Cumulant	Sys. Uncertainties (0-5%)
$C_1$	6%
$C_2$	5%
$C_3$	7%
$C_4$	22%

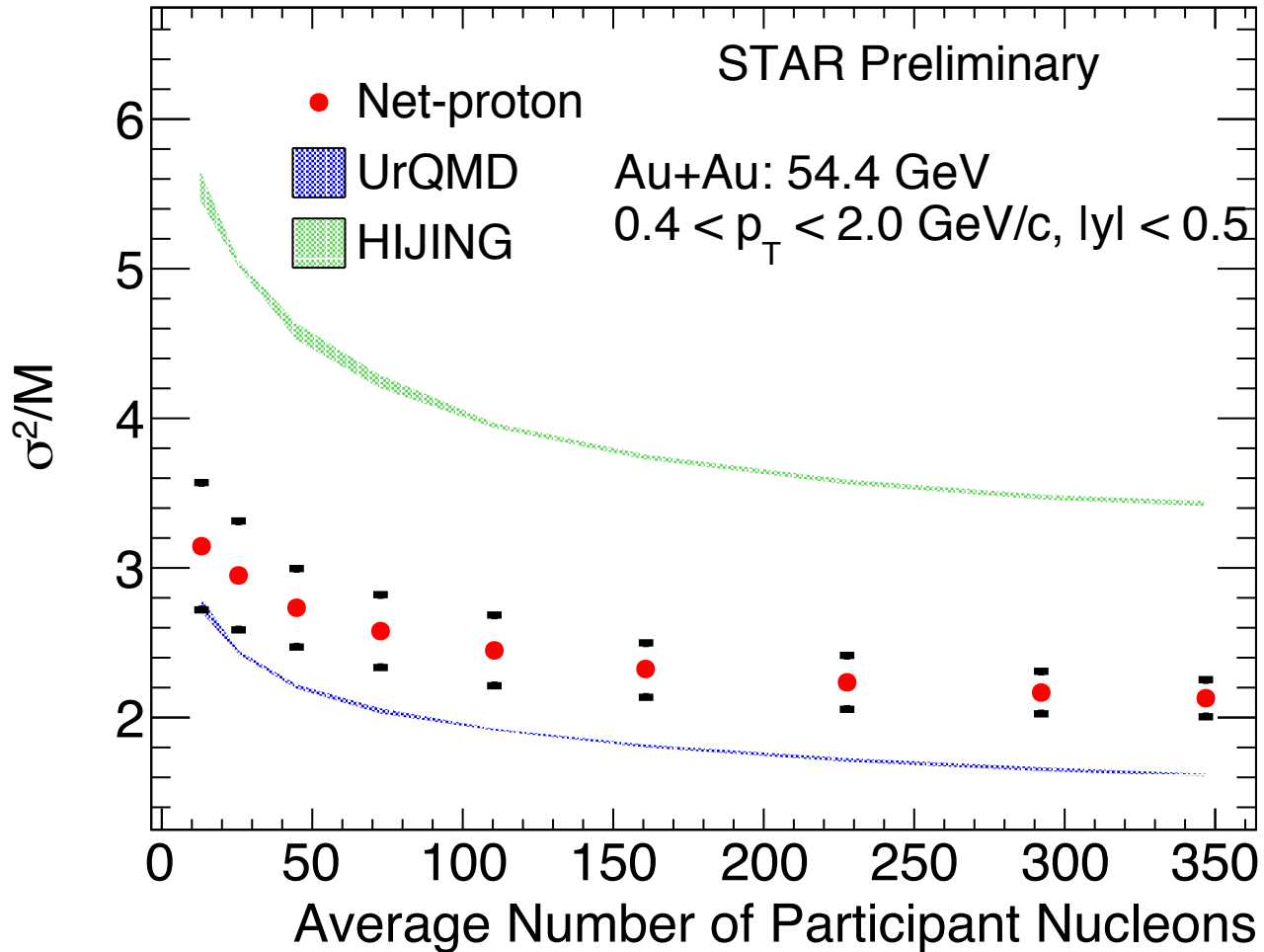


# Centrality Dependence of Cumulants



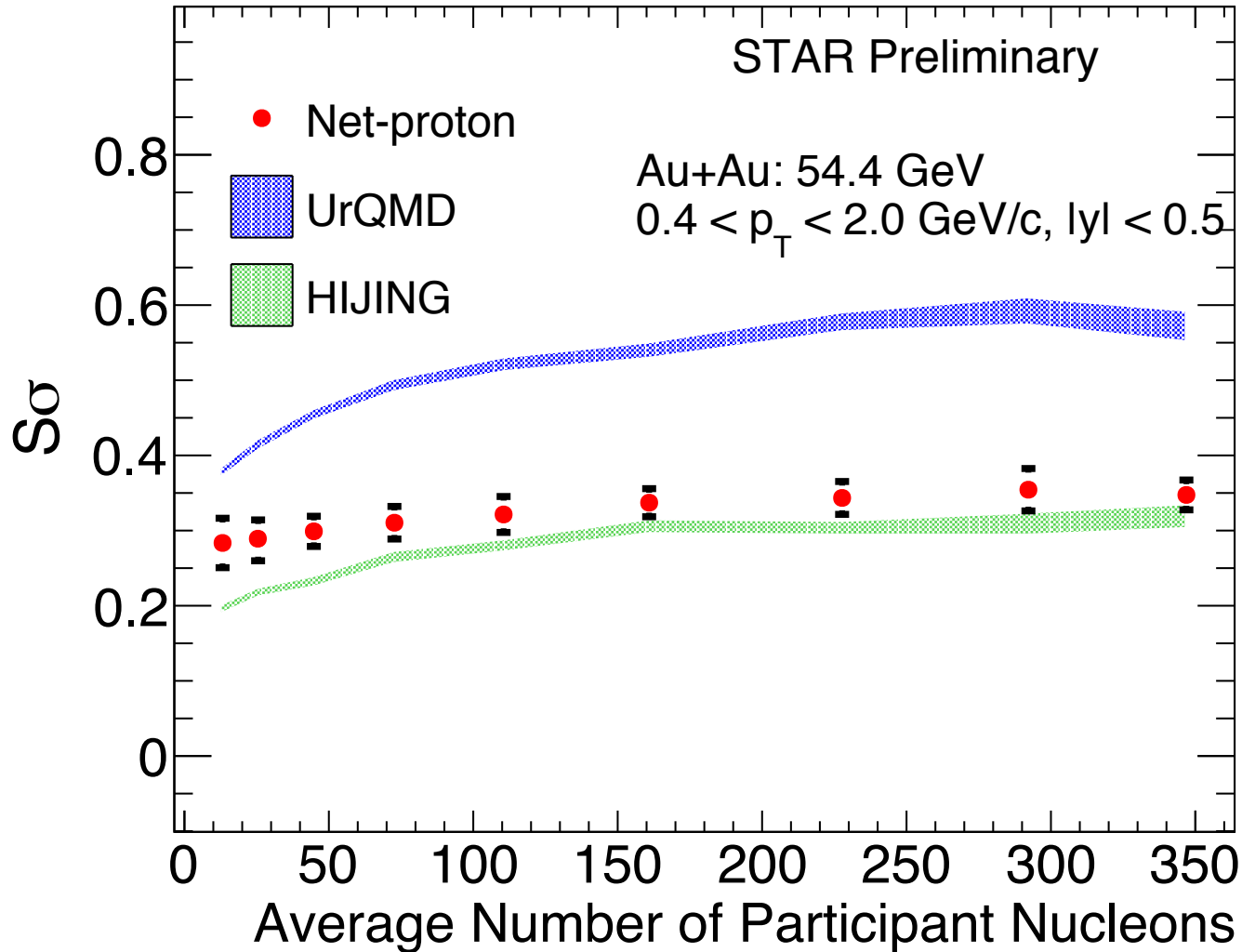
Net-proton cumulants up to the fourth order increases with number of participant nucleons

# Centrality Dependence of Cumulants Ratios



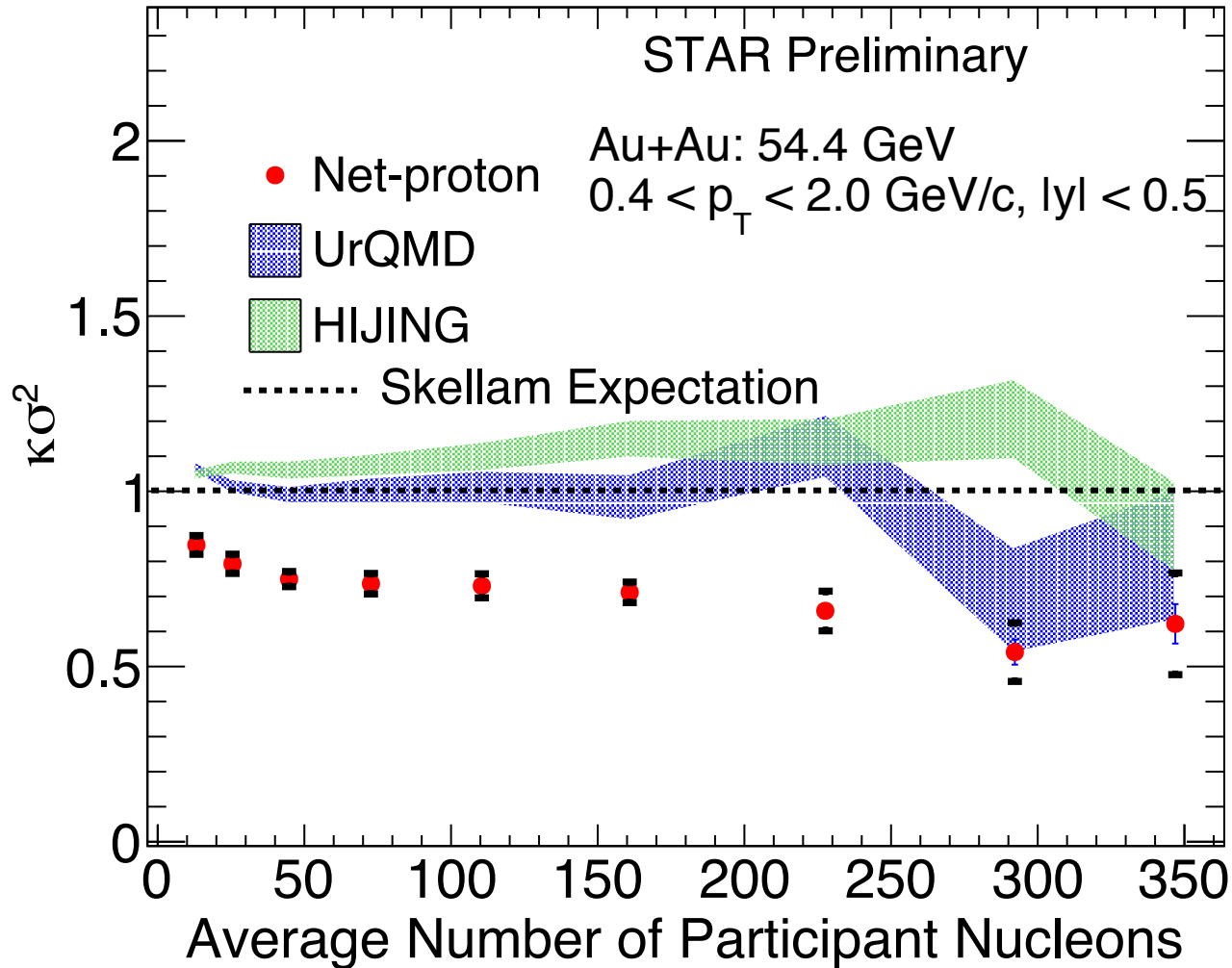
Net-proton cumulants ratio  $C_2/C_1$  variation with number of participant nucleons. Results compared to the UrQMD and HIJING model calculations

# Centrality Dependence of Cumulants Ratios



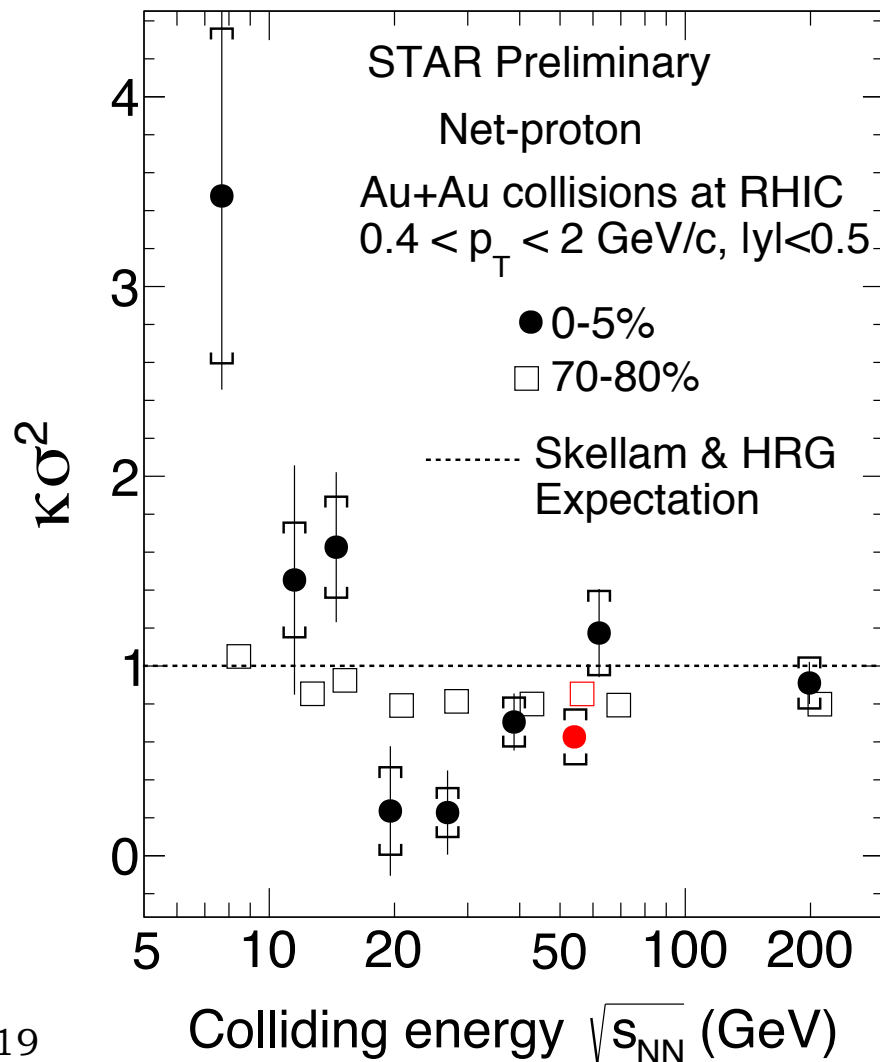
Net-proton cumulants ratio  $C_3/C_2$  variation with number of participant nucleons. Results compared to the UrQMD and HIJING model calculations

# Centrality Dependence of Cumulants Ratios



Net-proton cumulants ratio  $C_4/C_2$  variation with number of participant nucleons. Results compared to the UrQMD and HIJING model calculations

# Energy Dependence of Cumulant Ratios



STAR: Xiaofeng Luo,  
PoS CPOD2014 (2015) 019

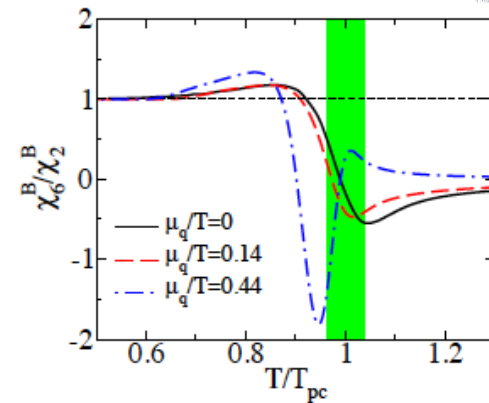
Dependence of net-proton cumulants ratio  $C_4/C_2$  on beam energy including results from 54.4 GeV.

# The Sixth-Order Cumulant



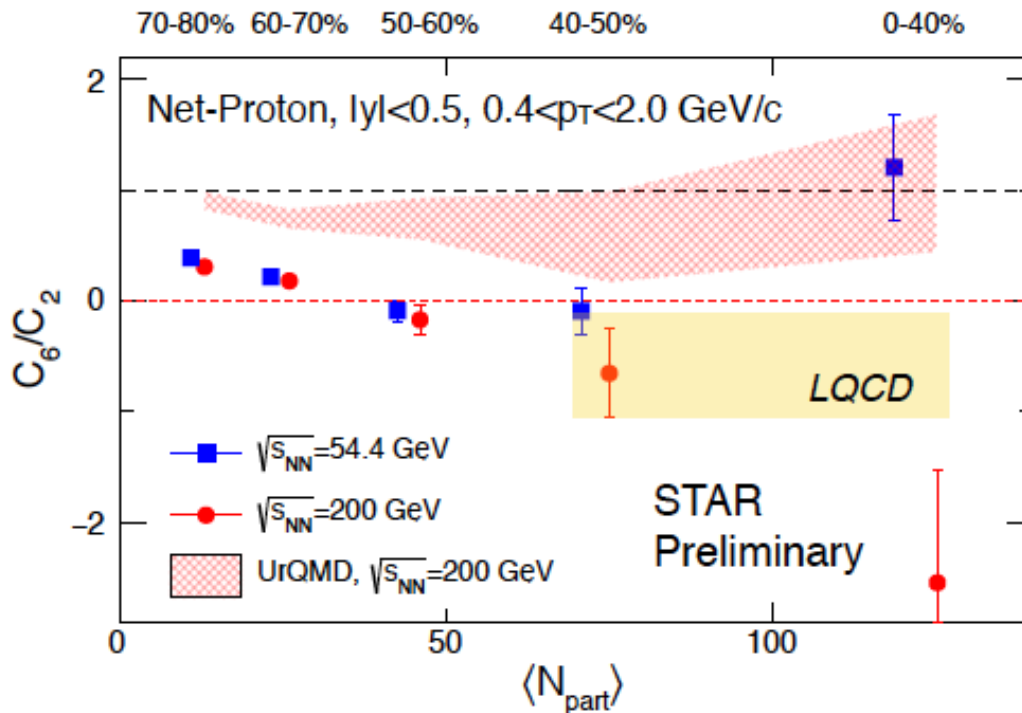
Goal: Identification of O(4) chiral criticality on the phase boundary.

freeze-out conditions	$\chi_4^B/\chi_2^B$	$\chi_6^B/\chi_2^B$	$\chi_4^Q/\chi_2^Q$	$\chi_6^Q/\chi_2^Q$
HRG	1	1	$\sim 2$	$\sim 10$
QCD: $T^{\text{freeze}}/T_{pc} \lesssim 0.9$	$\gtrsim 1$	$\gtrsim 1$	$\sim 2$	$\sim 10$
QCD: $T^{\text{freeze}}/T_{pc} \simeq 1$	$\sim 0.5$	$< 0$	$\sim 1$	$< 0$



The sixth-order cumulants of baryon number and electric charge fluctuations remain negative at the chiral transition temperature.

Most central value of  $C_6/C_2$   
 $C_6/C_2 < 0$  for  $\sqrt{s_{NN}} = 200$  GeV  
 $C_6/C_2 > 0$  for  $\sqrt{s_{NN}} = 54.4$  GeV

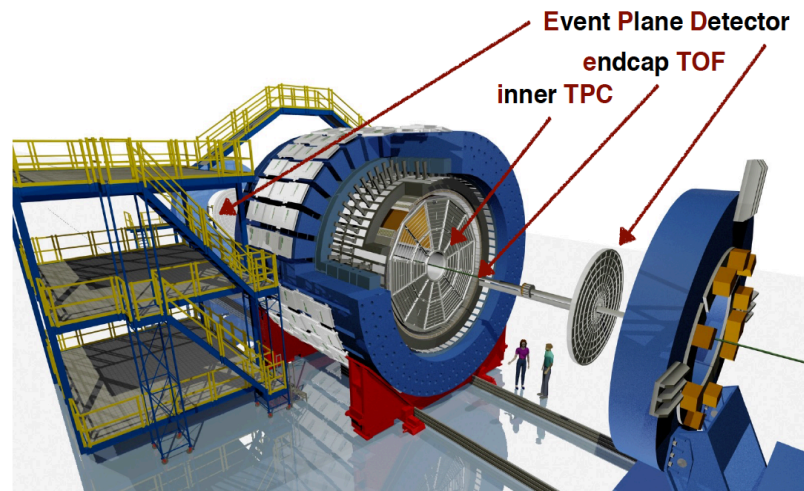


# Summary



- ❑ The first measurements of net-proton cumulants (up to the fourth order) presented for Au+Au collisions at  $\sqrt{s_{NN}} = 54.4$  GeV. Measurements carried out at midrapidity ( $|y| < 0.5$ ), wide transverse momentum range ( $0.4 < p_T < 2.0$  GeV/c) and nine centrality bins.
- ❑ The cumulants monotonically increase with increasing number of participant nucleons.
- ❑ The  $C_2/C_1$  shows a strong centrality dependence, whereas  $C_3/C_2$  and  $C_4/C_2$  have a weak centrality dependence.
- ❑ The centrality dependence of cumulant ratios is only qualitatively reproduced by the UrQMD and HIJING models. Quantitative differences exist.
- ❑ The  $C_6/C_2$  for central Au+Au collisions at 54.4 GeV is positive while that for 200 GeV is negative (with large uncertainties). These have consequences vis-à-vis chiral criticality in QCD.

# Beam Energy Scan Phase - II



$\sqrt{s}$ (GeV)	Statistics(Millions) – BES-I	Statistics(Millions) – BES-II
7.7	~4	~ <b>100</b>
9.1	-	~ <b>160</b>
11.5	~12	~ <b>230</b>
14.5	~ 20	~ <b>300</b>
19.6	~36	~ <b>400</b>
27	~70	~ <b>500</b>

iTPC	EPD	eTOF
Larger rapidity coverage $ \eta  < 1.5$	$2.1 <  \eta  < 5.1$	$-1.6 < \eta < 1.0$
Better $dE/dx$ resolution	Better Centrality determination	PID extended to forward rapidity
Lower momentum acceptance $> 0.1$ GeV/c	Better event plane resolution	
Physics Impact: Higher moments and Dilepton	Physics Impact: Higher moments, $v_n$	Physics Impact: Fixed target program and all analysis with PID